Available online at www.sciencedirect.com
SCIENCE DIRECT®
Biochemical and Biophysical Research Communications 323 (2004) 583–591
BBRC
www.elsevier.com/locate/ybbrc

Optimal construction of non-immune scFv phage display libraries from mouse bone marrow and spleen established to select specific scFvs efficiently binding to antigen

Takayuki Okamoto[a,1], Yohei Mukai[a,1], Yasuo Yoshioka[a,b,1], Hiroko Shibata[a], Maki Kawamura[a], Yoko Yamamoto[a], Shinsaku Nakagawa[a], Haruhiko Kamada[d], Takao Hayakawa[b], Tadanori Mayumi[c], Yasuo Tsutsumi[a,d,*]

[a] *Department of Biopharmaceutics, Graduate School of Pharmaceutical Sciences, Osaka University, 1-6 Yamadaoka, Suita, Osaka 565-0871, Japan*
[b] *National Institute of Health Sciences (NIHS), 1-18-1, Kamiyoga, Setagaya-ku, Tokyo 158-8501, Japan*
[c] *Department of Cell Therapeutics, Graduate School of Pharmaceutical Sciences, Kobe Gakuin University, 518 Arise, Ikawadani, Nishiku, Kobe 651-2180, Japan*
[d] *National Institute of Health Sciences, Osaka Branch Fundamental Research Laboratories for Development of Medicine, 7-6-8 Saito-Asagi, Ibaraki, Osaka 567-0085, Japan*

Received 20 May 2004

Abstract

Monoclonal antibodies (MAbs) are widely applied in basic research, medicine, and the pharmaceutical industry. Recently, applications and generations of MAbs have been increasingly attracting attention in many research areas since MAbs could be produced in large quantities with the development of genetic technology and antibody engineering. On the other hand, in recent years, phage display system has been developed for high-throughput isolation and generation of novel MAbs that have high affinity with various antigens. This technology is capable of constructing "Library" containing billions of phage repertoires displaying various antibody fragments, and rapid selection of a specific MAb from this phage library. Additionally, this technology has a great advantage that MAbs can be generated without immunization to animals. However, there are still relatively few reports confirming that useful MAbs can be derived from non-immune antibody libraries. The latter, as undertaken by current methods, seem unable to achieve the high quality required to produce useful MAbs for any desired antigen because cloning of antibody gene from non-immune donors is inefficient. This problem is caused by the fact that their RT-PCR primer sets, PCR conditions, and efficiency of subcloning through construction of antibody gene library cannot encompass all the antibody diversity. In an attempt to overcome some of these earlier problems, here we describe an optimized method to establish a high quality, non-immune library from mouse bone-marrow and spleen, and assess its diversity in terms of content of multiple antibodies for a wide antigenic repertoire. As an example of the application of the methodology, we describe the selection of specific MAbs binding to Luciferase and identify at least 18 different clones. Using this non-immune mouse antibody library, we also obtained MAbs for VEGF, VEGF receptor 2, TNF-α, and *Pseudomonas* Exotoxin, confirming the high quality of the library and its suitability for this application.

Keywords: Phage display system; Non-immune library; Antibody therapy

Monoclonal antibodies (MAbs) are essential tools in molecular biology, clinical examinations, medical treatment of cancer, infectious diseases, and in many other areas [1–3]. MAbs are routinely generated from mice

* Corresponding author. Fax: +81 6 6879 8178.
E-mail addresses: tsutsumi@phs.osaka-u.ac.jp, ytsutsumi@nihs.go.jp (Y. Tsutsumi).
[1] These authors contributed equally to the work.

0006-291X/$ - see front matter © 2004 Elsevier Inc. All rights reserved.
doi:10.1016/j.bbrc.2004.08.131

or rats using hybridoma technology [4,5], which involves immunizing the animal with a target antigen, isolating the relevant B cells, and fusing them with immortal cell lines to create antibody-producing hybridoma cells. Typically, in order to generate MAbs for a particular antigen, a number of mice are immunized over a period of 2–6 months, followed by a further 1–2 months of laboratory work before the hybridoma cells can be finally produced.

In contrast, the phage display system represents a more rapid technique, because it does not require immunizing the donor with antigen and avoids much laborious laboratory work. Using phage display system, various antibody fragments can be displayed on the surface of filamentous phages containing the antibody gene as a phagemid [6–9]. On the other hand, antibody fragments including scFv (single-chain fragment variable) molecules have been developed for potential clinical applications [10–12]. ScFvs, smallest antibody fragments, are composed of a light chain and a heavy chain variable region (VL and VH, respectively) joined via a short peptide spacer sequence. Thus, the phage display system has been developed from recombinant scFv techniques for the cloning and expression of cDNAs encoding the variable regions of antibody VL and VH chains and allows the in vitro generation of large antibody repertoires [13]. The processes required for this phage display system, i.e., RT-PCR, and PCR amplification and selection from phages displaying combinatorial libraries, constitute a selection step analogous to that occurring during the primary immune response. These processes allow the in vitro construction of antibody fragments of diverse specificities. The selection of non-immune libraries can yield a set of recombinant scFvs within 2–3 weeks. Moreover, a critical advantage of this technology is the direct link that exists between the experimental phenotype and its encapsulated genotype. This technology allows the evolution of the selected binders into optimized molecules, by affinity maturation via hot spot mutation [14,15] and enhancing in vivo stability by lowering the p*I* effect [16].

Use of such antibody libraries from non-immune donors has enabled the identification of MAbs in rapid high-throughput mode; however, successful initial construction of the non-immune libraries has thus far been achieved only by a small number of research groups [17,18]. In addition, non-immune libraries constructed by current methods lack the full variable region gene repertoire and show low efficiency of generation and creation of scFv gene diversity. In other words, previous methods for library construction are unable to encompass all potential antibody gene repertoires, because the primer set for cloning the VH and VL genes is not satisfactory. Additionally, PCR amplification conditions, efficiency of ligation of scFv gene to vector, and conditions employed for phage antibody secretion are all very important factors for establishing a large non-immune library. Establishing non-immune antibody libraries of high quality and great diversity under optimized conditions is needed.

In this study, we optimized the above-mentioned conditions to establish a high quality non-immune library, with a large size that potentially includes many specificities present in vivo. We describe the production of a mouse non-immune library based on optimized conditions including the nature of the primer sets for cloning antibody repertoires, PCR and ligation conditions, and phage production. By way of illustration, 18 specific monoclonal scFvs were selected from this library on the basis of binding to Luciferase, a model antigen. Detailed analysis of the anti-Luciferase scFvs confirmed their specificity and sequence. To demonstrate the general efficacy of our approach, we selected specific scFvs binding to diverse antigens, namely, vascular endothelial growth factor (VEGF), VEGF receptor 2 (VEGF-R2), tumor necrosis factor-alpha (TNF-α), and *Pseudomonas* Exotoxin (PE). This optimized methodology permits the construction of a high quality phage library easily and it can be applied to the development of phage display systems.

Materials and methods

Construction of non-immune mouse scFv phage libraries. Fig. 1 is a flow diagram that shows the construction of a non-immune mouse scFv phage library. Total RNA was prepared from spleen tissue and bone marrow of non-immunized 6-week-old male C57BL/6, Balb/c, and C3H mice. Mouse mRNA was purified using oligo(dT) columns (Amersham–Pharmacia Biotech, Uppsala, Sweden) and subsequently first strand cDNA was generated using Superscript II reverse transcriptase (Invitrogen, Carlsbad, CA). From each cDNA, heavy- and light-chain genes were amplified separately and recombined by three subsequent PCRs. In the first-step PCR, the heavy- and light-chains were amplified. The light chain 5′ primers were modified to include an *Sfi*I site, and heavy chain 3′ primers to include a *Not*I site. Light chain 3′ primers were designed to assemble with heavy chain 5′ primers (Tables 1 and 2). Heavy and light chain variable region genes were amplified by PCR containing 2 μL cDNA and 25 pmol of each 5′ and 3′ primer, using the Expand High Fidelity PCR system (Roche Diagnostics, Indianapolis, IN, USA). The samples were cycled 35 times at 96 °C for 60 s, 55 °C for 60 s, and 68 °C for 60 s. The samples were then purified from the agarose gel by GenElute MINUS EtBr Spin Columns (Sigma Chemical, St. Louis, MO). In the second-step PCR, heavy and light chains were assembled. The first-step PCR products of heavy and light chains were mixed, and the assembly PCR containing equal amounts of the products was cycled 20 times at 96 °C for 60 s, 63 °C for 60 s, and 68 °C for 60 s without primers. The samples were purified with QIAquick PCR Purification Kits (QIAGEN, Valencia, CA). The third-step PCR extended the second PCR products by overlap PCR. This PCR extends the scFv gene (second-PCR products) using the following primers: the Y15 primer (5′-gcc aag ctt tgg agc ctt ttt ttt gga gat ttt caa cgt gaa aaa att att att cgc aat tcc ttt agt tgt tcc ttt cta tgc ggc cca gcc ggc cat ggc c-3′) and the Y16 primer (5′-cgc cgg cgt cca cgc ggc cac ggc ata ggc cta ggc gac ctt ggc gca cgg cgt atc tga caa ctt tca aca aat cgt ttt gga gta tgt ctt tta agt aaa tg-3′). The modified 5′ primer and 3′ primer are were extended from the *Sfi*I

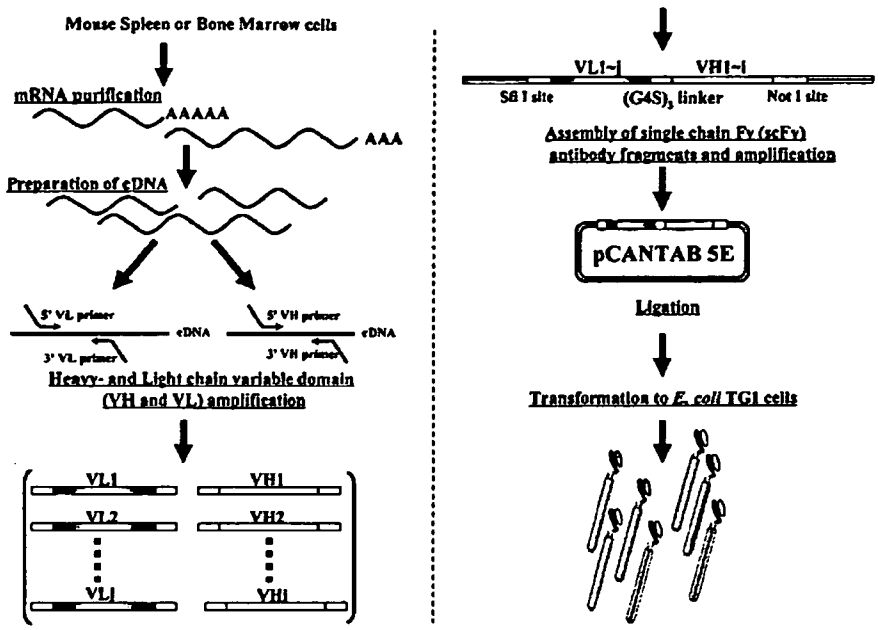

Fig. 1. Flow diagram illustrating construction of the scFv phage library.

Table 1
Primers for PCR amplification of mouse antibody light chain variable regions

VL-5′ primers	5′-cct ttc tat gcG GCC CAG CCG GCC atg gcc GAY ATT GTD HTV WCH CAG TC-3′
	5′-cct ttc tat gcG GCC CAG CCG GCC atg gcc GAY ATT NWK MTV AHD CAG TC-3′
	5′-cct ttc tat gcG GCC CAG CCG GCC atg gcc GAY RTY BWR MTS ACM CAR WC-3′
	5′-cct ttc tat gcG GCC CAG CCG GCC atg gcc GAY ATY SWG MTG ACN CAR BC-3′
	5′-cct ttc tat gcG GCC CAG CCG GCC atg gcc GAY RYT GTK RTR MYY MRG DW-3′
VL-3′ primers	5′-acc aga gcc gcc gcc gcc gct acc acc acc acc CCG TTY NAK YTC CAR CTT DG-3′
	5′-acc aga gcc gcc gcc gcc gct acc acc acc acc MCS TWB NAB HKY CAV YYT DG-3′

S = G/C, R = G/A, K = G/T, M = A/C, Y = C/T, W = A/T, H = A/C/T, B = C/G/T, V = A/C/G, D = A/G/T, and N = A/T/G/C.

Table 2
Primers for PCR amplification of mouse antibody heavy chain variable regions

VH-5′ primers	5′-agc ggc ggc ggc ggc tct ggt ggt ggt gga tcc SAK GTB MAG CTB MAG SAS TC-3′
	5′-agc ggc ggc ggc ggc tct ggt ggt ggt gga tcc SAG GTY CAR CTB CAR CAR TC-3′
	5′-agc ggc ggc ggc ggc tct ggt ggt ggt gga tcc SAV GTS MWS BTG RWG SAR TC-3′
	5′-agc ggc ggc ggc ggc tct ggt ggt ggt gga tcc GAK GTG MAV SKG RTG GAR TC-3′
	5′-agc ggc ggc ggc ggc tct ggt ggt ggt gga tcc GAR GTR MAR STT SWB GAG TC-3′
	5′-agc ggc ggc ggc ggc tct ggt ggt ggt gga tcc SAK GTB MMN YTV VWV SWR YS-3′
VH-3′ primers	5′-cgg cac cgg cgc acc tGC GGC CGC YGA RGA RAC DST GAS MRK RGT-3′
	5′-cgg cac cgg cgc acc tGC GGC CGC YGA RGA RRM SKK KAS WGW GRT-3′
	5′-cgg cac cgg cgc acc tGC GGC CGC YGA GGA GAC KGT GAS HGD GGH-3′

S = G/C, R = G/A, K = G/T, M = A/C, Y = C/T, W = A/T, H = A/C/T, B = C/G/T, V = A/C/G, D = A/G/T, N = A/T/G/C.

and *Not*I sites of scFv genes upstream by overlap PCR. The third overlap PCR was run under the same cycling conditions as the first-PCR at an annealing temperature of 65 °C.

Cloning of the mouse scFv repertoire into pCANTAB 5E. The PCR-amplified scFv DNAs and pCANTAB 5E phagemid vector were digested with *Not*I and *Sfi*I. The resulting scFv fragments were inserted into pCANTAB 5E phagemid vector to generate an scFv-gene III fusion library, using T4 ligase (Roche Diagnostics, Indianapolis, IN, USA) at 16 °C for 16 h. Ligated DNA populations were introduced into *Escherichia coli* (*E. coli*) TG1 using a Bio-Rad Gene Pulser (Bio-Rad Laboratories, CA). Each library was then grown by culturing at 37 °C in 2-YT medium, supplemented with ampicillin (100 μg/mL) and

glucose (2% w/v). Colonies were then collected, mixed with glycerol, and stored at −80 °C. Panning of phage particles was done as described earlier. Phage preparations were purified and concentrated by polyethylene glycol (PEG) precipitation.

Selection of anti-Luciferase antibodies. A large mouse scFv phage display library containing 5×10^8 clones was used for the selection. The library stock was grown in log phase, rescued with M13KO7 helper phage (Invitrogen, Carlsbad, CA), and amplified overnight in 2YTAK (2YT containing 100 μg/mL ampicillin and 50 μg/mL kanamycin) at 37 °C. The phage was precipitated with 4% PEG/0.5 M NaCl, resuspended in NTE buffer (100 mM NaCl, 10 mM Tris, and 1 mM EDTA) and incubated with 2% Block Ace at 4 °C for 1 h to block nonspecific binding. Immunotubes (Nunc maxisorp; Life Technologies, Merelbeke, Belgium) were coated with 10 μg/mL Luciferase (Promega, Madison, WI), TNF-α, VEGF-R2, VEGF or PE in carbonate/bicarbonate buffer (Sigma Chemical, St. Louis, MO). Prior to this, they were first blocked with 2% Block Ace at 4 °C for 1 h. Then the tubes were incubated with phage preparation at 4 °C for 1 h. After incubation, the tubes were washed 10 times with PBST (PBS containing 0.05% Tween 20) and subsequently with PBS. The bound phage was eluted at 4 °C for 10 min with 1 mL of freshly prepared 100 mM HCl solution. The eluted phage particles were incubated with 10 mL of log phase TG1 cells at 37 °C with shaking at 110 rpm for 20 min and at 250 rpm for 30 min. The infected cells were mixed with glycerol at −80 °C. For the next round of panning, 3 mL of infected TG1 cell stock was added to 50 mL of 2YTAG medium and grown to log phase. The culture was rescued with M13KO7 helper phage, amplified, precipitated, and used for selection, following the procedure described earlier. The panning process was repeated.

Phage ELISA. After the panning process, individual TG1 clones were picked, grown at 37 °C in 96-well plates, and rescued with M13KO7 helper phage as described earlier. The amplified phage preparation was blocked with 2% Block Ace at 4 °C for 1 h and then added to Maxi-sorp 96-well microtiter plates coated with Luciferase or ovalbumin (10 μg/mL, SIGMA). After overnight incubation at 4 °C, the plates were washed three times with PBST and PBS, and incubated with a mouse anti-M13 phage-horseradish peroxidase (HRP) conjugate (Amersham–Pharmacia Biotech, Uppsala, Sweden). The plates were washed three times, TMB peroxidase substrate was added, and the absorbance was read at 450 nm using a microplate reader (Bio-Rad Laboratories, CA).

DNA BstNI pattern analysis and nucleotide sequencing. After the third round of panning, the diversity of the selected scFv clones was analyzed by restriction enzyme digestion patterns (i.e., DNA fingerprint analysis). The scFv gene insert of individual clones was amplified by PCR using the following primers: pCANTAB5-S1 primer (5′-cag gaa aca gct atg ac-3′) and pCANTAB5-S6 primer (5′-gta aaa cga cga cgg cca gt-3′). The amplified product was digested with a frequent-cutting enzyme, *Bst*NI (NEB), and analyzed on agarose gels. DNA sequencing was performed using the BigDye Terminator Ready Reaction Kit (Applied Biosystems).

Results and discussion

In this study, we present the principle of selecting specific scFv for any antigen from a non-immune mouse scFv library (Fig. 1). For the construction of these large libraries, mRNA was extracted from mouse bone marrow and spleen cells, and the cDNA fragments encoding VL and VH genes were amplified by RT-PCR. In previous methods, the VL and VH genes were not adequately

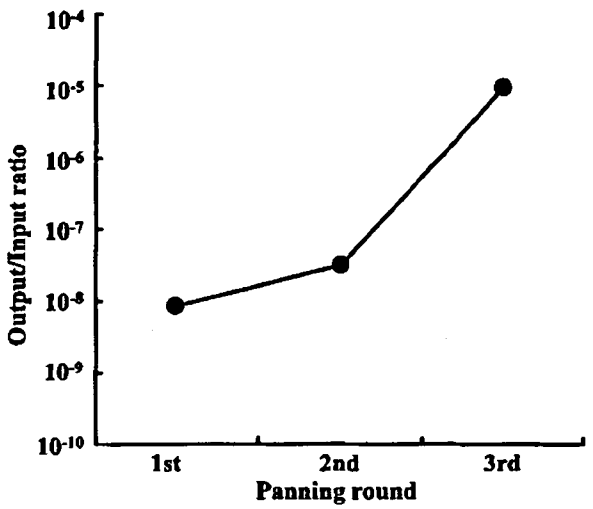

Fig. 3. Selection of phage-scFv libraries by panning in immunotubes. Luciferase-coated immunotubes were first blocked with 2% Block Ace at 4 °C for 1 h and then incubated with phage preparations at 37 °C for 1 h. The tubes were washed 10 times with PBST (PBS containing 0.05% Tween 20) followed by PBS. The bound phage was eluted with 1 mL of freshly prepared 100 mM HCl solution at 4 °C for 10 min. The ratio was calculated as follows: (output phage titer)/(input phage titer). The second and third panning input phage preparations were amplified from the last rounds of the output phages.

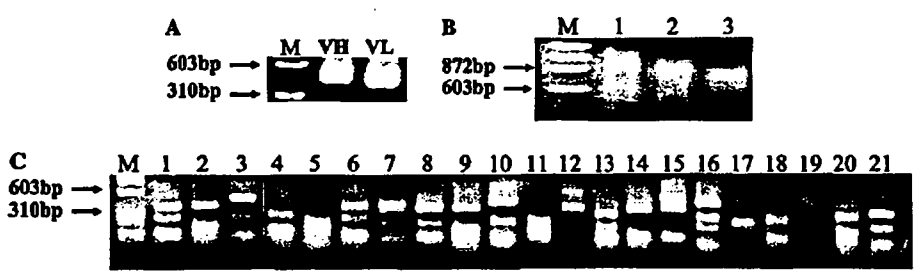

Fig. 2. Construction of non-immune mouse scFv library. (A) The amplified variable regions of heavy- and light-chains from mouse bone marrow and spleen. (B) Preparation of scFv genes. Lane 1, third PCR products; lane 2, scFv genes digested with *Sfi*I; and lane 3, scFv genes digested with *Not*I. (C) Non-immune scFv encoding inserts of 21 phage clones were amplified by PCR using pCANTAB5-S1 and pCANTAB5-S6 primers. The amplified products were digested with the frequent-cutting enzyme *Bst*NI at 60 °C for 2 h. The restriction patterns of samples were analyzed on agarose gels.

and accurately amplified, because the RT-PCR was not run under optimal conditions. This step is dependent on several factors, of which the most critical is the diversity of primer sets covering the whole VL and VH gene repertoires. In contrast, we have constructed original primer sets that encompass theoretical whole repertoires using The Kabat Database [19] and previous report [20] as reference (Tables 1 and 2). In fact, in control comparative experiments, we were unable to amplify scFv genes even from the OKT9, W6/32, and TES23 hybridomas using previous primer sets [20] (data not shown). On the other hand, using our modified primer sets (Tables 1 and 2), the VL and VH genes were clearly amplified at 340 and 400 bp from these hybridomas. Moreover, in this step, the use of high fidelity *Taq* polymerase as well as the Expand High Fidelity PCR system, and specific primer sets, resulted in better coverage of the mouse antibody gene repertoire. In each case, PCR amplification using our improved primer sets yielded sufficient amounts of products of the predicted size, as shown by a sharp band (Fig. 2A). This result suggested that our primer sets possess sufficient diversity for constructing comprehensive non-immune scFv libraries.

Table 3
Selection of scFv displaying phage binding to Luciferase

Panning rounds	1st	2nd	3rd
Total input phage (CFU)	3.1×10^{11}	6.6×10^{11}	1.5×10^{12}
Total output phage (CFU)	2.7×10^{3}	2.1×10^{4}	1.4×10^{7}
Ratio (output phage/input phage)	8.7×10^{-9}	3.2×10^{-8}	9.3×10^{-6}

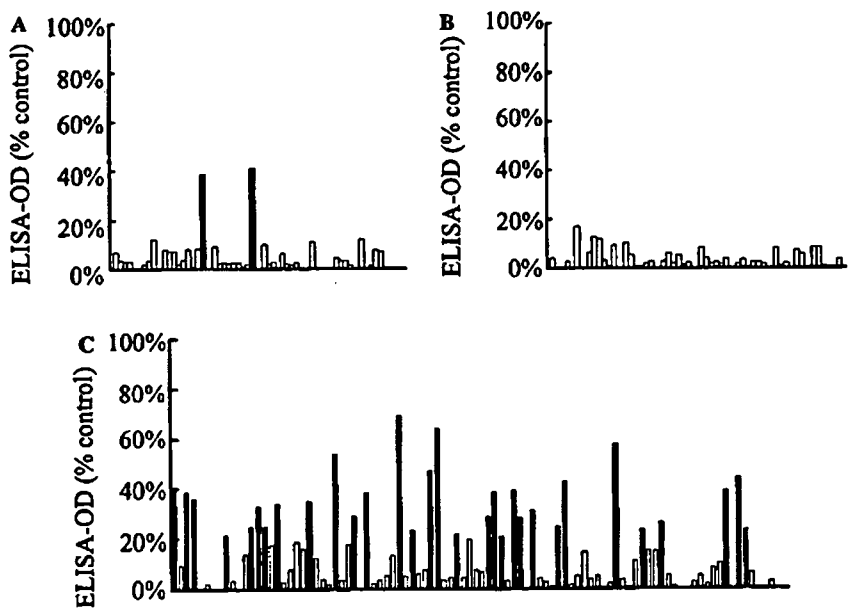

Fig. 4. Binding activity to Luciferase of output phage clones. After panning on Luciferase, the binding properties of selected clones were measured by ELISA. (A) Forty-eight clones from the first panning output phages, (B) 42 clones from the second panning output phages, and (C) 90 clones from the third panning output phages. Percentage control was (sample OD/positive control OD) × 100%. The positive control was the wild-type phage captured by anti-M13 Mab and detected by anti-M13 Mab HRP conjugate.

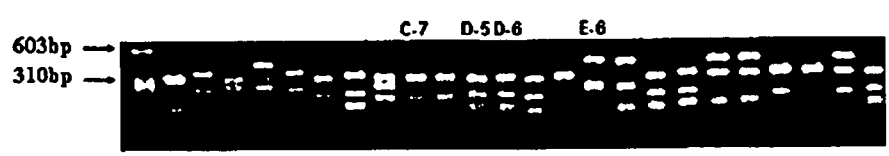

Fig. 5. Fingerprint analysis of anti-Luciferase scFvs. Anti-Luciferase scFv-encoding inserts of 21 phage clones were amplified by PCR using pCANTAB5-S1 and pCANTAB5-S6 primers. The amplified products were digested with the frequent-cutting enzyme *Bst*NI at 60 °C for 2 h. The restriction patterns of samples were analyzed on agarose gels.

In order to create scFv fragment genes (Fig. 1), 3′ ends of VL genes were fused to 5′ ends of VH genes through a $(G4S)_3$ linker peptide, and the VL and VH genes were assembled and amplified. We constructed VL-linker-VH-type scFv genes such that the 3′ end of the light chain was complementary to the 5′ end of the linker and the 3′ end of this linker DNA was in turn complementary to the 5′ end of the heavy chain. The scFv genes of the third PCR products were digested by *Sfi*I and *Not*I, and the bands obtained were trimmed of elongation sequences (Fig. 2B). By traditional methods, only a restricted repertoire of mouse antibody genes can be amplified and ligated using the pCANTAB5E vector. However, this method is not efficient, because scFv genes are commonly too short to be cut with some enzymes, i.e., in general, the sequences at the 5′ and 3′ ends of the PCR products are too short. To overcome this problem, we extended the 5′ end of VL and 3′ end of VH by approximately 100 bp at the third PCR, and improved the efficiency of cutting following the ligation step. The VH-linker-VL-type scFv formed by the inversion of VL and VH genes had lower affinity and bioactivity than the VL-linker-VH-type scFvs, which were created from an anti-TNF-α MAb-secreting hybridoma.

A combinatorial non-immune mouse scFv library of 5×10^8 clones was established by cloning the scFv fragments into a vector, which allowed the fusion of the heavy chain variable fragment to gene III protein of phage minor coat protein. To ascertain the scFv repertoire and the quality of the non-immune antibody library, DNA segments encoding the scFv genes from 21 randomly picked clones were identified from the primary library. These clones were amplified and digested with *Bst*NI, and their fingerprint patterns were compared. The patterns of these clones were found to vary, indicating an excellent diversity in the non-immune mouse scFv library (Fig. 2C). Using this method, we succeeded in establishing a non-immune mouse scFv library, which demonstrated a large diversity of scFv, and we also confirmed that our non-immune scFv phage library was composed of billions of independent clones.

In general, in order to select useful specific scFv antibodies for target antigens, it is important that the primary phage libraries demonstrate high quality. The term "high quality" implies several key features. Importantly, the library must have a large functional size to match diverse antibody sequences to facilitate the selection of a variety of high affinity scFvs. It is essential that the scFv genes be well expressed to allow the panning process. In this study, we established a large non-immune scFv phage display library and attempted to isolate specific scFvs for firefly Luciferase as a model antigen. Phage clones binding to immobilized Luciferase were selected on the basis of their affinity as described in Materials and methods. Fig. 3 shows the enrichment and screening of the phage scFv antibody library. The vertical axis indicates the ratio

Table 4
Amino acids sequence of anti-Luciferase scFv

Clone name	FR1	CDR1	FR2	CDR2	FR3	CDR3	FR4	(G4S)3
	VL							
C-7	DIQMMQSTSSLSAS	RTSQDIN	WYQQKPDG	YTSRL HS	GVPSRFSGSGSGTDYSLTISNL	QQGNTL	FGAGTK	GGGGSGGGGS
	LGDRVTISC	YLN	TVKLLIY		EQEDIATYFC	PLT	LELKR	GGGS
D-5	DIVITQSPAILSVSP	RASQSIG	WYQQRTNG	YASESIS	GIPSRFSGSGSGTDFTLSINSVE	QQSNSW	FGAGTK	GGGGSGGGGS
	GERVSFSC	TSIH	SPRLLIE		SEDIADYYC	PTT	LTVL	GGGS
D-6	DIQMTQSPVILSVSP	RASQSIG	WYQQRING	YASES IS	RIPSRFSGSGSGTDFTLSINSVE	QQSNSW	FGAGTK	GGGGSGGGGS
	EGERVSFSC	TSIH	PPRPLIK		SEDIADYYC	PALT	LEIKR	GGGS
E-6	DILLTASPVILSVSP	RASQNI	WYQQRING	YASESIS	RIPSRFSGSGSGTDFTLTINSVE	QQSNSW	FGAGTK	GGGGSGGGGS
	GERVSFSC	GTSIH	SPRLLIK		SEDIADYYC	PALT	LEIKR	GGGS
	VH							
C-7	EVMLVESGPELVKPGASVKISC	SYWMN	WMKQRPG	QIYPGDGET	KATLTADKSSTAYMQLSS	FDGYYVD	WGQGT	
	KASGYTFS		KGLEWIG	NTNGKFKG	LTSEDSAVTFCAS	Y	TLQSS	
D-5	QVQLQQSGPELARPWASVKISC	RRVHFAIR	WVKQRPG	AIYPGNGDT	KALTLTADKSSSTAYMQLS	DPLVY	WGQGT	
	QAFYTFS	DTNYWMQ	QGLEWIG	SYNQKFKG	SLTSEDSAVYFCAR		TLTVSS	
D-6	QVKVKQSGAKLVKPGAAVKVS	SYWMH	WVKQRPG	QIYPGDGDT	KALTLTVDKSSSTAYMQLTS	QSSYVFDY	WGQGT	
	CKASGYTFT		HGLEWIG	NTNGEFKG	SLTSEDSAVYFCAS		TLTVSS	
E-6	EVQLQQSGPELVKPGASVKISC	DYNMN	WVKQSNG	VINPNYGTTS	KALTLTVDQSSSTAYMQLS	ENYYGSSY	WGQGT	
	KASGYSFT		KSLEWIG	YNQKFKG	SLTSEDSAVYYCTR	LYYAMKDY	TVTVSS	

of the number of recovered phages from the immunotube to the number of phages added. At the second round of panning, there was a 3-fold increase in enrichment, which was again increased approximately 300-fold by the third round. Thus, the overall enrichment was approximately 1000-fold (Table 3). These results suggest that high affinity scFv-displayed phage clones could be selected from the scFv library by affinity panning.

A total of three rounds of selection was performed on immobilized Luciferase. After each round, a total of 180 clones was randomly picked and their binding to Luciferase was tested by phage ELISA (Fig. 4). A few clones after the second selection and 31 clones after the third were positive for Luciferase binding. And then, we also confirmed that soluble formed scFvs of them could bind to Luciferase as well (data not shown). These results suggest high efficiency of the selection process. Additionally, crossreactivity on ovalbumin-immobilized phage ELISA demonstrated that 29 of the 31 scFvs were specific Luciferase binders (data not shown). DNA segments encoding the scFvs from 21 binders, identified in the third selection, were amplified, digested with *Bst*NI, and their fingerprint patterns were compared. A total of 18 different patterns was identified among the 21 clones, indicating an excellent diversity of the isolated anti-Luciferase scFvs (Fig. 5). Partial DNA sequencing data further confirmed that four clones were unique, with different nucleotide and amino acid sequences (Table 4). The fingerprints of clones D-5 and D-6 clones were apparently identical, although their amino acid sequences were different. Therefore, we have accomplished the generation of at least 18 different anti-Luciferase scFv antibody clones.

The large mouse scFv library was established in order to isolate multiple scFv binding to any antigen. To determine the general diversity of the scFv library, it was subjected to three rounds of selection on four different antigens, namely, immobilized VEGF, VEGF-receptor, TNF-α, and PE. After three rounds of selection, the ratio of the number of recovered selected phages from the immunoadsorption tubes to the number of phages added increased from 5- to 1000-fold (Fig. 6). In all cases, the scFv genes from randomly picked clones were analyzed by fingerprinting, and a unique pattern of scFv genes was identified from the non-immune mouse scFv library. Hence, we have succeed in establishing a non-immune mouse library, with a large functional size and a high antibody sequence diversity in order to facilitate the selection of a variety of high affinity scFvs. Further, it was essential that the scFv genes be well-expressed to allow for efficient panning.

In the last decade, recombinant antibody engineering has emerged as one of the most promising approaches for the design, selection, and production of reagents for basic research, medicine, and the pharmaceutical industry [21–23]. The in vitro selection and evolution of phage libraries now provide us with very powerful tools for producing antibodies without using animals and the immune system. Significant advances in the past decade with phage and other display methodologies,

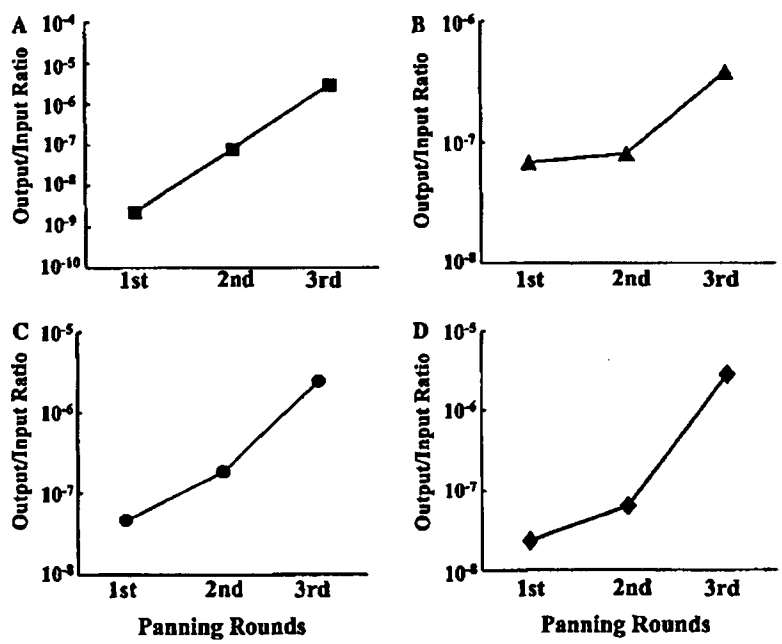

Fig. 6. Selection of phage-scFv libraries by panning. Selection on various antigens was performed by panning in antigen-coated immunotubes with (A) VEGF-receptor2, (B) VEGF, (C) TNF-α, and (D) PE.

library design, refined selection procedures, and instrumentation for automation have made display technologies increasingly popular for creating antibodies to be used in all areas of research, and also for medical and industrial applications. In the present study, we have explored the generation of useful antibodies such as cell type- and tissue-specific binders for application as cell markers and drug delivery carriers, by biopanning with cell and tissue in vivo. Moreover, to create more useful antibodies, we developed a novel modified methodology using polyethylene glycol to improve the stability and antigenicity of the antibodies. Previously, we reported that the site-specific modification of polyethylene glycol to protein improves the stability and other characteristics without deactivation of bioactivity [24]. Recently, we have used a number of such antibodies in clinical applications, and given their availability, these methodologies were used to develop antibody therapy to explore novel antibodies from the library and to improve their characteristics to make them more suitable as clinical tools. We believe that antibody therapy will be more widely applied in future and that this will be facilitated by the use of improved techniques for their production, such as those described here.

Acknowledgments

This study was supported in part by Grants-in-Aid for Scientific Research (No.15680014 and No.16023242) from the Ministry of Education, Culture, Sports, Science and Technology of Japan; a Health and Labor Sciences Research Grant from the Ministry of Health, Labor and Welfare of Japan; Health Sciences Research Grants for Research on Health Sciences focusing on Drug Innovation from the Japan Health Sciences Foundation; the Takeda Science Foundation; the Senri Life Science Foundation; and by JSPS Research Fellowships for Young Scientists (No. 08476).

References

[1] G.L. Plosker, D.P. Figgitt, Rituximab: a review of its use in non-Hodgkin's lymphoma and chronic lymphocytic leukaemia, Drugs 63 (2003) 803–843.

[2] F. Baert, M. Noman, S. Vermeire, G. Van Assche, D.H. G, A. Carbonez, P. Rutgeerts, Influence of immunogenicity on the long-term efficacy of infliximab in Crohn's disease, N. Engl. J. Med. 348 (2003) 601–608.

[3] D.J. Slamon, B. Leyland-Jones, S. Shak, H. Fuchs, V. Paton, A. Bajamonde, T. Fleming, W. Eiermann, J. Wolter, M. Pegram, J. Baselga, L. Norton, Use of chemotherapy plus a monoclonal antibody against HER2 for metastatic breast cancer that overexpresses HER2, N. Engl. J. Med. 344 (2001) 783–792.

[4] G. Kohler, H. Hengartner, M.J. Shulman, Immunoglobulin production by lymphocyte hybridomas, Eur. J. Immunol., 8 (1978) 82–88.

[5] W. Gerhard, C.M. Croce, D. Lopes, H. Koprowski, Repertoire of antiviral antibodies expressed by somatic cell hybrids, Proc. Natl. Acad. Sci. USA 75 (1978) 1510–1514.

[6] A.D. Griffiths, M. Malmqvist, J.D. Marks, J.M. Bye, M.J. Embleton, J. McCafferty, M. Baier, K.P. Holliger, B.D. Gorick, N.C. Hughes-Jones, et al., Human anti-self antibodies with high specificity from phage display libraries, EMBO J. 12 (1993) 725–734.

[7] H. Gram, L.A. Marconi, C.F. Barbas 3rd, T.A. Collet, R.A. Lerner, A.S. Kang, In vitro selection and affinity maturation of antibodies from a naive combinatorial immunoglobulin library, Proc. Natl. Acad. Sci. USA 89 (1992) 3576–3580.

[8] T. Clackson, H.R. Hoogenboom, A.D. Griffiths, G. Winter, Making antibody fragments using phage display libraries, Nature 352 (1991) 624–628.

[9] G.P. Smith, Filamentous fusion phage: novel expression vectors that display cloned antigens on the virion surface, Science 228 (1985) 1315–1317.

[10] R.H. Begent, M.J. Verhaar, K.A. Chester, J.L. Casey, A.J. Green, M.P. Napier, L.D. Hope-Stone, N. Cushen, P.A. Keep, C.J. Johnson, R.E. Hawkins, A.J. Hilson, L. Robson, Clinical evidence of efficient tumor targeting based on single-chain Fv antibody selected from a combinatorial library, Nat. Med. 2 (1996) 979–984.

[11] J.C. Fitch, S. Rollins, L. Matis, B. Alford, S. Aranki, C.D. Collard, M. Dewar, J. Elefteriades, R. Hines, G. Kopf, P. Kraker, L. Li, R. O'Hara, C. Rinder, H. Rinder, R. Shaw, B. Smith, G. Stahl, S.K. Sherman, Pharmacology and biological efficacy of a recombinant, humanized, single-chain antibody C5 complement inhibitor in patients undergoing coronary artery bypass graft surgery with cardiopulmonary bypass, Circulation 100 (1999) 2499–2506.

[12] K.W. Mahaffey, C.B. Granger, J.C. Nicolau, W. Ruzyllo, W.D. Weaver, P. Theroux, J.S. Hochman, T.G. Filloon, C.F. Mojcik, T.G. Todaro, P.W. Armstrong, Effect of pexelizumab, an anti-C5 complement antibody, as adjunctive therapy to fibrinolysis in acute myocardial infarction: the COMPlement inhibition in myocardial infarction treated with thromboLYtics (COMPLY) trial, Circulation 108 (2003) 1176–1183.

[13] A.D. Griffiths, A.R. Duncan, Strategies for selection of antibodies by phage display, Curr. Opin. Biotechnol. 9 (1998) 102–108.

[14] P.S. Chowdhury, I. Pastan, Improving antibody affinity by mimicking somatic hypermutation in vitro, Nat. Biotechnol. 17 (1999) 568–572.

[15] R. Beers, P. Chowdhury, D. Bigner, I. Pastan, Immunotoxins with increased activity against epidermal growth factor receptor vIII-expressing cells produced by antibody phage display, Clin. Cancer Res. 6 (2000) 2835–2843.

[16] M. Onda, S. Nagata, Y. Tsutsumi, J.J. Vincent, Q. Wang, R.J. Kreitman, B. Lee, I. Pastan, Lowering the isoelectric point of the Fv portion of recombinant immunotoxins leads to decreased nonspecific animal toxicity without affecting antitumor activity, Cancer Res. 61 (2001) 5070–5077.

[17] T.J. Vaughan, A.J. Williams, K. Pritchard, J.K. Osbourn, A.R. Pope, J.C. Earnshaw, J. McCafferty, R.A. Hodits, J. Wilton, K.S. Johnson, Human antibodies with sub-nanomolar affinities isolated from a large non-immunized phage display library, Nat. Biotechnol. 14 (1996) 309–314.

[18] S. Goletz, P.A. Christensen, P. Kristensen, D. Blohm, I. Tomlinson, G. Winter, U. Karsten, Selection of large diversities of antiidiotypic antibody fragments by phage display, J. Mol. Biol. 315 (2002) 1087–1097.

[19] The Kabat Database of Sequences of Proteins of Immunological Interest. Available from: <http://www.kabatdatabase.com>.

[20] A. Krebber, S. Bornhauser, J. Burmester, A. Honegger, J. Willuda, H.R. Bosshard, A. Pluckthun, Reliable cloning of functional antibody variable domains from hybridomas and

spleen cell repertoires employing a reengineered phage display system, J. Immunol. Methods 201 (1997) 35–55.
[21] J.S. Ross, K. Gray, G.S. Gray, P.J. Worland, M. Rolfe, Anticancer antibodies, Am. J. Clin. Pathol. 119 (2003) 472–485.
[22] R.P. Valle, M. Jendoubi, Antibody-based technologies for target discovery, Curr. Opin. Drug. Discov. Dev. 6 (2003) 197–203.
[23] M.G. Russeva, G.P. Adams, Radioimmunotherapy with engineered antibodies, Expert. Opin. Biol. Ther. 4 (2004) 217–231.
[24] Y. Yamamoto, Y. Tsutsumi, Y. Yoshioka, T. Nishibata, K. Kobayashi, T. Okamoto, Y. Mukai, T. Shimizu, S. Nakagawa, S. Nagata, T. Mayumi, Site-specific PEGylation of a lysine-deficient TNF-alpha with full bioactivity, Nat. Biotechnol. 21 (2003) 546–552.

Effective accumulation of poly(vinylpyrrolidone-*co*-vinyl laurate) into the spleen

Yasuo Yoshioka, Yasuo Tsutsumi, Yohei Mukai, Hiroko Shibata, Takayuki Okamoto, Yoshihisa Kaneda, Shin-ichi Tsunoda, Haruhiko Kamada, Keiichi Koizumi, Yoko Yamamoto, Yu Mu, Hiroshi Kodaira, Keiko Sato-Kamada, Shinsaku Nakagawa, Tadanori Mayumi

Department of Biopharmaceutics, Graduate School of Pharmaceutical Sciences, Osaka University, 1-6 Yamadaoka, Suita, Osaka 565-0871, Japan

Received 12 January 2004; accepted 26 February 2004
Published online 8 June 2004 in Wiley InterScience (www.interscience.wiley.com). DOI: 10.1002/jbm.a.30059

Abstract: To optimize polymer-conjugated drugs as a polymeric drug delivery system, it is essential to design polymeric carriers with tissue-specific targeting capacity. Previously, we showed that polyvinylpyrrolidone (PVP) was the most suitable polymeric carrier for prolonging the blood-residency of drugs, and was one of the best parent polymers to design the polymeric carriers with targeting capacity. In this study, we synthesized some hydrophobic PVP derivatives, poly(vinylpyrrolidone-*co*-styrene) [poly(VP-*co*-S)] and poly(vinylpyrrolidone-*co*-vinyl laurate) [poly(VP-*co*-VL)], and assessed their biopharmaceutical properties after intravenous administration in mice. The elimination of hydrophobic PVP derivatives from blood was the same as PVP, and the plasma half-lives of poly(VP-*co*-S) were almost similar to that of poly(VP-*co*-VL). Poly(VP-*co*-VL) efficiently accumulated in the spleen, whereas poly(VP-*co*-S) effectively accumulated in the liver. The level of poly(VP-*co*-VL) in the spleen was about 20 times higher than PVP and poly(VP-*co*-S). These hydrophobic PVP derivatives did not show any cytotoxicity against endothelial cells *in vitro*. Thus, poly(VP-*co*-VL) may be a useful polymeric carrier for drug delivery to the spleen. This study will provide useful information to design optimal polymeric carriers with targeting capacity to the spleen and liver. © 2004 Wiley Periodicals, Inc. J Biomed Mater Res 70A: 219–223, 2004

Key words: polymeric carrier; drug delivery system; targeting; polyvinylpyrrolidone; hydrophobic

INTRODUCTION

Because of recent advances in structural genomics and pharmacoproteomics, the functions of numerous proteins can be clarified. The therapeutic application of bioactive proteins, such as newly identified proteins and cytokines, is also expected.[1–4] Because these proteins are generally quite unstable *in vivo*, their clinical application requires frequent administration at high dosages. This often results in impaired homeostasis *in vivo* and may lead to severe adverse effects. Because cytokines such as interleukin (IL)-2 and tumor necrosis factor (TNF)-α have diverse effects on various tissues, it is not easy to selectively obtain a favorable function (therapeutic effects) of such proteins among their diverse functions to minimize their side effects.[5] The same problems exist in antitumor chemotherapeutic agents and immunosuppressive drugs.[6] To overcome these problems, we attempted to conjugate bioactive proteins with nonionic polymeric carriers such as polyethylene glycol (PEG).[7–11] Chemical conjugation of proteins with PEG, as a polymeric drug delivery system (DDS), increases their molecular size and enhances steric hindrance, both of which are dependent on the PEG attached to the protein. This results in improving the plasma half-lives of proteins and their stability against proteolytic cleavage, as well as a decrease in their immunogenicity. We also reported that PEGylation of proteins such as TNF-α, IL-6, and immunotoxins could enhance therapeutic potency and reduce undesirable effects.

For further improvement of this polymeric DDS, it is essential to design polymer-conjugated proteins with targeting capacity to the optimal tissue such as spleen and kidney. It is well known that the fate and

Correspondence to: Y. Tsutsumi; e-mail: tsutsumi@phs.osaka-u.ac.jp

Contract grant sponsor: Ministry of Education, Science and Culture of Japan (Grant-in-Aid for Scientific Research); contract grant number: 15680014
Contract grant sponsor: Japan Health Sciences Foundation (Health Sciences Research Grants for Research on Health Sciences Focusing on Drug Innovation); contract grant number: KH63124
Contract grant sponsor: Takeda Science Foundation

distribution of the polymer-conjugated proteins can be attributed to the physicochemical properties of polymeric carriers such as molecular weight, electric charge, and hydrophilic–lipophilic balance. Therefore, to control the *in vivo* behavior of conjugated proteins with polymeric carriers, it is necessary to assess the pharmacokinetic characteristics of the polymeric carriers themselves. Previously, we showed that polyvinylpyrrolidone (PVP) had much longer circulation time than PEG, which has been used for bioconjugation (PEGylation) frequently, and tissue distribution of PVP was markedly restricted.[12] Therefore, we found that PVP was the most feasible polymeric modifier for increasing the half-life of cytokines and retention in the circulation. For example, bioconjugation of TNF-α with PVP showed 200 times higher antitumor effects than native TNF-α with decreased side effects and the antitumor effects of PVP-modified TNF-α was two times higher than that of PEG-modified TNF-α.[9] Our other studies on IL-6 yielded similar results.[13] In addition, it is easy to introduce various comonomers on radical polymerization to PVP for giving new function such as targeting capacity. For instance, we found that anionized PVP derivatives selectively accumulated into the urinary organ.[14] Briefly, carboxylated PVP efficiently accumulated in the kidney, whereas sulfonated PVP was rapidly excreted in the urine. Thus, these carboxylated and sulfonated PVPs may be useful polymeric carriers for drug delivery to kidney and bladder, respectively. Recently, we synthesized a novel polymeric drug carrier, polyvinylpyrrolidone-*co*-dimethyl maleic anhydride [poly(VP-*co*-DMMAn)], for its application in a renal DDS. About 80% of poly(VP-*co*-DMMAn) selectively accumulated in the kidneys 24 h after iv administration.[10] Poly(VP-*co*-DMMAn)-conjugated superoxide dismutase (SOD) accumulated in the kidneys after iv administration, and accelerated recovery from acute renal failure in a murine model. In contrast, PVP-modified SOD and native SOD were not as effective. These results suggested that PVP was the most feasible parent polymer for design of a novel polymeric carrier with targeting capacity.

In this study, we focused on assessing the *in vivo* behavior of hydrophobic PVP derivatives. To evaluate the relationship between pharmacokinetics and their hydrophobic functional groups, we synthesized poly(vinylpyrrolidone-*co*-styrene) [poly(VP-*co*-S)] and poly(vinylpyrrolidone-*co*-vinyl laurate) [poly(VP-*co*-VL)] by radical copolymerization. We found that poly(VP-*co*-VL) was useful for the targeting carrier to the spleen and poly(VP-*co*-S) was useful for the targeting carrier to the liver. This study is the first report of creation of the targeting carrier to the spleen. This study may provide useful information, which will facilitate the optimal molecular design of polymeric drug carriers applicable to therapeutic use for DDS to the spleen and liver.

MATERIALS AND METHODS

Materials

Chemicals were purchased from Wako Pure Chemical Industries Ltd. (Osaka, Japan). TSKgel G4000PW and TSKgel alpha-3000 columns were obtained from Tosoh Corporation (Tokyo, Japan). $Na^{125}I$ (3.7 GBq/mL) solution was obtained from NEN Research Products (Boston, MA).

Animals and cells

All experimental protocols for animal studies were in accordance with the Guide for Laboratory Animal Facilities and Care (National Institutes of Health publication 85-23, rev. 1985). These protocols have been approved by the committee at the school of Pharmaceutical Science, Osaka University. Male ddY mice were obtained from SLC (Hamamatsu, Japan). Sarcoma-180 cells (S-180; Cancer Cell Repository Institute of Development, Aging and Cancer, Tohoku University) were maintained intraperitoneally through serial passages in ddY mice.

Synthesis of PVP and its hydrophobic derivatives

PVP was synthesized by the radical polymerization method using 4,4'-azobis-4-cyanovaleric acid and β-mercaptopropionic acid as radical initiator and chain transfer agent, respectively. The hydrophobic PVP derivatives of both poly(VP-*co*-S) and poly(VP-*co*-VL) were prepared by radical copolymerization of VP and hydrophobic comonomers (styrene or vinyl laurate) in dimethylformamide with the aid of 4,4'-azobis-4-cyanovaleric acid and mercaptopropionic acid as for PVP. These polymers were separated into several fractions by gel filtration chromatography (GFC) to obtain polymers with a narrow molecular weight distribution. The number-average molecular weight of PVP and both hydrophobic PVP derivatives was about 10 kDa (polydispersity $[M_w/M_n]$ <1.39; PEG standards). The comonomer content determined by ^1H NMR was in good agreement with the feed molar ratio of the hydrophobic comonomer relative to the VP monomer.

In vivo behavior of polymers

^{125}I-radiolabeled polymers were prepared by the chloramine-T method and purified by GFC. The specific activities of ^{125}I-labeled polymers were about 4.44 μCi/mg/polymer. S-180 cells were implanted intradermally (5×10^5 cells/200 μL/site) in mice that were injected iv with ^{125}I-labeled poly-

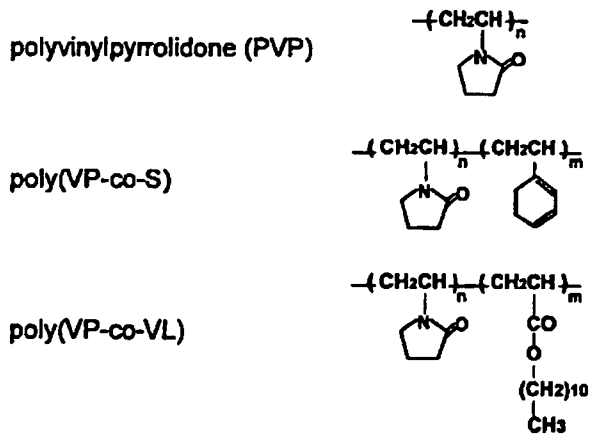

Figure 1. Chemical structures of PVP and hydrophobic PVP derivatives.

mer (1×10^6 cpm/200 μL) 7 days later when the diameter of the tumors exceeded 7 mm. Blood was collected from the tail vein at intervals and radioactivity was measured. GFC analysis confirmed that there was more than 95% of radioactivity in the circulating blood, 3 h after iv injection was derived from the intact ^{125}I-labeled polymers.

Pyrene fluorescence assay

Various concentrations of polymer solutions were added to each vial containing $1.0 \times 10^{-7}M$ pyrene and heated for 1 h at 70°C to equilibrate the pyrene and the polymers. Emission spectra of pyrene were recorded on a spectrofluorometer (excitation at 336 nm) and the intensity of emission peaks at 382 and 392 nm was determined.

RESULTS

Plasma clearance

The hydrophobic PVP derivatives, poly(VP-*co*-S) and poly(VP-*co*-VL), were synthesized by radical polymerization methods (Fig. 1). These products were separated and purified by GFC to adjust the molecular size (10 kDa) and polydispersity of PVP. We confirmed the successful synthesis of these products by NMR. These hydrophobic PVP derivatives at a dose of 10 mg/mL did not show any cytotoxicity against endothelial cells *in vitro* (data not shown). The plasma clearance of PVP and the hydrophobic PVP derivatives were compared after iv injection in mice bearing S-180 solid tumors (Fig. 2). Pharmacokinetics of ^{125}I-labeled polymers was not influenced by the ^{125}I-labeling method and the preparative method for activated polymers (data not shown). Additionally, almost all radioactivity in the blood was derived from the ^{125}I-labeled polymers by GFC analysis, 3 h after iv injection (data not shown). Therefore, it was considered that the pharmacokinetics of ^{125}I-labeled polymers was exactly correlated with that of the polymers. All polymers showed biphasic elimination patterns. Both poly(VP-*co*-S) and poly(VP-*co*-VL) as well as PVP, showed long retention in circulation and 25% of the injected dose remained in circulation after 180 min.

Tissue distribution

Next, we studied the tissue distribution of the polymers 3 h after iv injection (Fig. 3). Each polymer, with the same molecular weight, showed a characteristic distribution. PVP showed little tissue-specific localization. Poly(VP-*co*-S) (S: 1%) did not demonstrate specific tissue accumulation as well as PVP. However, poly(VP-*co*-S) (S: 3%) tended to accumulate in the liver, whereas the accumulation of poly(VP-*co*-S) (S: 3%) in other organs was similar to poly(VP-*co*-S) (S: 1%). In contrast, poly(VP-*co*-VL) effectively accumulated in spleen and accumulated more than 20 times higher than PVP or poly(VP-*co*-S) (S: 1%).

Detection of conformational shift of the polymers by pyrene fluorescence assay

In general, hydrophobic polymers tend to assemble each other in water. Therefore, the difference of phar-

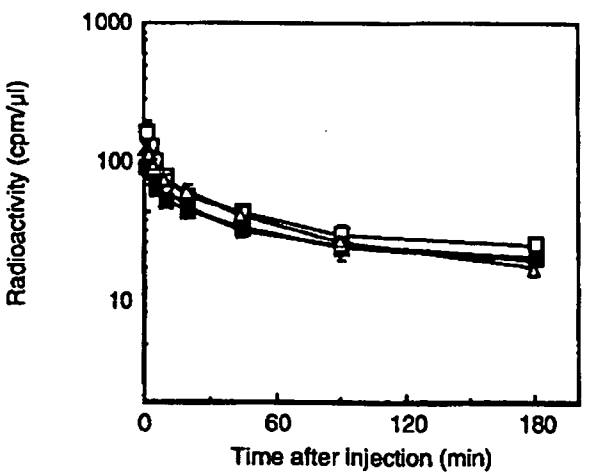

Figure 2. Plasma clearance of PVP and hydrophobic PVP derivatives after iv injection in mice. Mice were intravenously injected with ^{125}I-labeled polymers. After administration, blood was collected at indicated times and radioactivity was measured using a γ-counter. Mice were used in groups of five. Each value is the mean ± standard error. (○) PVP; (□) poly(VP-*co*-S) (S: 1%); (■) poly(VP-*co*-S) (S: 3%); (△) poly(VP-*co*-VL) (VL: 1%).

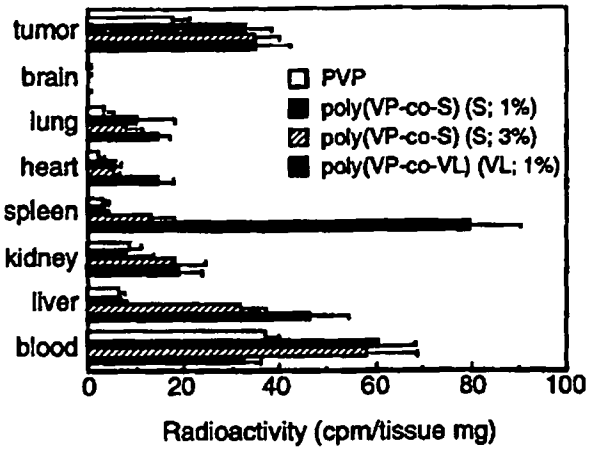

Figure 3. Tissue distribution of PVP and hydrophobic PVP derivatives at 3 h after iv injection in mice. At 3 h after iv injection, mice were killed and each organ was collected. The radioactivity was measured using a γ-counter. Mice were used in groups of five. Each value is the mean ± standard error.

macokinetics of the hydrophobic PVP derivatives would result from the difference of the state of the polymer in blood. Fluorescence probe technique was used to investigate the self-assembly of the polymers in water using pyrene as a hydrophobic probe.[15] The transition from an expanded, hydrophilic coiled polymer to a compact, globular structure can be detected in the presence of pyrene as the change of the ratio of the emission intensity at 372 nm to that at 382 nm. Phosphatidylcholine, as a positive control, assembled with increase of the concentration. In contrast, no changes were detected in all hydrophobic PVP derivatives (Fig. 4).

DISCUSSION

Systemic administration of potential activators of immune cells for tumor or virus therapy such as IL-2, IL-12, and IFN-γ, or potential inhibitors of immune cells for autoimmune disease such as IL-10 and immunosuppressive drugs, has attracted much attention.[16] However, systemic administration of these cytokines is often associated with severe toxic side effects before the curative dose. To overcome these problems, it is important to develop an effective spleen DDS that selectively carries bioactive proteins to the spleen with a high degree of safety. In this regard, we previously reported that PVP was a more suitable polymeric carrier for enhancing the blood residency of drugs than PEG, which has been used frequently.[9,13] Using this PVP as a backbone polymer, we have evaluated the *in vivo* pharmacokinetics of synthesized PVP derivatives with various electrically charge or hydrophilic/hydrophobic balance.[10,14] For instance, the copolymer between VP and dimethyl maleic anhydride showed a marked increase in accumulation in the kidney.[10] In this study, we focused on the assessment of the *in vivo* behavior of hydrophobic PVP derivatives for optimizing the spleen DDS.

In vivo behavior of hydrophobic PVP derivatives was changed by type and content (molar ratio) of hydrophobic groups. Poly(VP-*co*-VL) and poly(VP-*co*-S), as well as PVP, showed high retention in circulation (Fig. 2). Furthermore, poly(VP-*co*-VL) accumulated in the spleen, as compared with other tissues such as the liver, kidney, and lung at 3 h after their iv injection (Fig. 3). The level of poly(VP-*co*-VL) in spleen was about 20-fold higher than PVP and poly(VP-*co*-S). However, poly(VP-*co*-S) showed little accumulation in the spleen. The reason for this difference is not clear, but it is partially due to the difference in structure of hydrophobic polymers. These results suggested that optimal hydrophobic groups may produce the highest accumulation in the spleen. The spleen is a lymphoid organ composed of red pulp and white pulp, containing T and B cell areas. The spleen has a unique vascular network and its framework is formed by a reticular meshwork consisting of fiber-forming reticular cells. The accumulation site of poly(VP-*co*-VL), and the mechanism of accumulation are currently under investigation. To evaluate the relationship between accumulation efficiency in the spleen and the number of vinyl laurate groups, we are synthesizing various

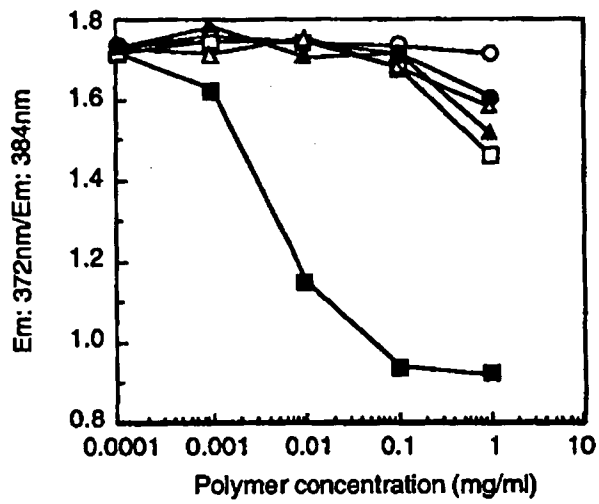

Figure 4. The ratio of pyrene emission intensity at 372 nm to that at 384 nm in the presence of poly(VP-*co*-S) and poly(VP)-*co*-VL. Pyrene and each polymer solution were mixed and incubated for 1 h at 70°C. After incubation, fluorescence activity (Ex: 336 nm, Em1: 372 nm, and Em3: 384 nm) was measured. (○) PEG; (•) PVP; (■) phosphatidylcholine; (▲) poly(VP-*co*-S) (S: 1%); (△) poly(VP-*co*-S) (S: 3%); (□) poly(VP-*co*-VL) (VL: 1%).

kinds of poly(VP-co-VL)s and examining the accumulation in the spleen. In addition, we are examining the therapeutic effects of poly(VP-co-VL) with immunosuppressive cytokine, IL-10, for the treatment of autoimmune diseases such as rheumatoid arthritis, and the usefulness of poly(VP-co-S) for the targeting carrier to liver is also under investigation.

This study may provide useful information that will facilitate the optimal molecular design of polymeric drug carriers applicable to therapeutic use for DDS to the spleen.

CONCLUSIONS

Both poly(VP-co-S) and poly(VP-co-VL), as well as PVP, showed long retention in circulation. Poly(VP-co-S) (S: 3%) tended to accumulate in the liver, whereas PVP showed little tissue-specific localization. Furthermore, poly(VP-co-VL) effectively accumulated in spleen and accumulated more than 20 times higher than PVP or poly(VP-co-S) (S: 1%).

References

1. Furman WL, Strother D, McClain K, Bell B, Leventhal B, Pratt CB. Phase I clinical trial of recombinant human tumor necrosis factor in children with refractory solid tumors: a Pediatric Oncology Group study. J Clin Oncol 1993;11:2205–2210.
2. Kreitman RJ, Wilson WH, Bergeron K, Raggio M, Stetler-Stevenson M, FitzGerald DJ, Pastan I. Efficacy of the anti-CD22 recombinant immunotoxin BL22 in chemotherapy-resistant hairy-cell leukemia. N Engl J Med 2001;345:241–247.
3. Glue P, Rouzier-Panis R, Raffanel C, Sabo R, Gupta SK, Salfi M, Jacobs S, Clement RP. A dose-ranging study of pegylated interferon alfa-2b and ribavirin in chronic hepatitis C. The Hepatitis C Intervention Therapy Group. Hepatology 2000;32: 647–653.
4. Barnard DL. Pegasys (Hoffmann-La Roche). Curr Opin Investig Drugs 2001;2:1530–1538.
5. Skillings J, Wierzbicki R, Eisenhauer E, Venner P, Letendre F, Stewart D, Weinerman B. A phase II study of recombinant tumor necrosis factor in renal cell carcinoma: a study of the National Cancer Institute of Canada Clinical Trials Group. J Immunother 1992;11:67–70.
6. Sparano JA. Doxorubicin/taxane combinations: cardiac toxicity and pharmacokinetics. Semin Oncol 1999;26:14–19.
7. Kaneda Y, Yamamoto Y, Kamada H, Tsunoda S, Tsutsumi Y, Hirano T, Mayumi T. Antitumor activity of tumor necrosis factor alpha conjugated with divinyl ether and maleic anhydride copolymer on solid tumors in mice. Cancer Res 1998;58: 290–295.
8. Tsutsumi Y, Onda M, Nagata S, Lee B, Kreitman RJ, Pastan I. Site-specific chemical modification with polyethylene glycol of recombinant immunotoxin anti-Tac(Fv)-PE38 (LMB-2) improves antitumor activity and reduces animal toxicity and immunogenicity. Proc Natl Acad Sci USA 2000;97:8548–8553.
9. Kamada H, Tsutsumi Y, Yamamoto Y, Kihira T, Kaneda Y, Mu Y, Kodaira H, Tsunoda SI, Nakagawa S, Mayumi T. Antitumor activity of tumor necrosis factor-alpha conjugated with polyvinylpyrrolidone on solid tumors in mice. Cancer Res 2000;60: 6416–6420.
10. Kamada H, Tsutsumi Y, Sato-Kamada K, Yamamoto Y, Yoshioka Y, Okamoto T, Nakagawa S, Nagata S, Mayumi T. Synthesis of a poly(vinylpyrrolidone-co-dimethyl maleic anhydride) co-polymer and its application as renal targeting carrier. Nat Biotechnol 2003;21:399–404.
11. Yamamoto Y, Tsutsumi Y, Yoshioka Y, Nishibata T, Kobayashi K, Okamoto T, Mukai Y, Shimizu T, Nakagawa S, Nagata S, Mayumi T. Site-specific PEGylation of a lysine-deficient TNF-alpha with full bioactivity. Nat Biotechnol 2003;21:546–552.
12. Kaneda Y, Tsutsumi Y, Yoshioka Y, Kamada H, Yamamoto Y, Kodaira H, Tsunoda S, Okamoto T, Mukai Y, Shibata H, Nakagawa S, Mayumi T. The use of PVP as a polymeric carrier to improve the plasma half-life of drugs. Biomaterials 2004;25: 3259–3266.
13. Tsunoda S, Kamada H, Yamamoto Y, Ishikawa T, Matsui J, Koizumi K, Kaneda Y, Tsutsumi Y, Ohsugi Y, Hirano T, Mayumi T. Molecular design of polyvinylpyrrolidone-conjugated interleukin-6 for enhancement of *in vivo* thrombopoietic activity in mice. J Control Release 2000;68:335–341.
14. Kodaira H, Tsutsumi Y, Yoshioka Y, Kamada H, Kaneda Y, Yamamoto Y, Tsunoda S, Okamoto T, Mukai Y, Shibata H, Nakagawa S, Mayumi T. The targeting of anionized polyvinylpyrrolidone to the renal system. Biomaterials 2004;25:4309–4315.
15. Yamamoto Y, Yasugi K, Harada A, Nagasaki Y, Kataoka K. Temperature-related change in the properties relevant to drug delivery of poly(ethylene glycol)-poly(D,L-lactide) block copolymer micelles in aqueous milieu. J Control Release 2002;82: 359–371.
16. van Deventer SJ, Elson CO, Fedorak RN. Multiple doses of intravenous interleukin 10 in steroid-refractory Crohn's disease. Crohn's Disease Study Group. Gastroenterology 1997; 113:383–389.

Gene Ther Mol Biol Vol 8, 163-172, 2004

The optimal molecular design of polymeric drug carriers and its application for renal drug targeting

Review Article

Takayuki Okamoto[1], Shinsaku Nakagawa[1], Yasuo Tsutsumi [1,2,*]

[1]Graduate School of Pharmaceutical Sciences, Osaka University, 1-6 Yamadaoka, Suita, Osaka 565-0871, Japan,
[2]National Institute of Health Sciences, Osaka Branch Fundamental Research Laboratories for Development of Medicine 1-1-43 Hoenzaka, Chuo-ku, Osaka 540-0006, Japan

*Correspondence: Yasuo Tsutsumi, Ph.D., Department of Biopharmaceutics, Graduate School of Pharmaceutical Sciences, Osaka University; 1-6 Yamadaoka, Suita, Osaka 565-0871, Japan; Phone and Fax: +81-(0) 6-6879-8178; E-mail: tsutsumi@phs.osaka-u.ac.jp

Key words: conjugation, PEGylation, polyethylene glycol, polyvinylpyrrolidone, dimethylmaleic acid, protein therapy

Abbreviations: Dimethyl maleic anhydride (DMMAn); immunotoxin (IT); interleukin-10 (IL-10); interleukin-6 (IL-6); poly(vinylpyrrolidone-co-dimethyl maleic acid), (PVD); polyacrylamide (PAAm); polydimethylacrylamide (PDAAm); polyethylene glycol (PEG); polyvinyl alcohol (PVA); polyvinylpyrrolidone (PVP); superoxide dismutase (SOD); tumor necrosis factor-a (TNF-a); vinylpyrrolidone (VP)

Received: 10 May 2004; Accepted: 14 May 2004; electronically published: May 2004

Summary

Renal disease is a serious health problem which is on the increase in the world. Over time such conditions necessitate dialysis and may require a kidney transplant. However these therapies are expensive and do not restore normal health. Therefore, new therapeutic strategies must be developed for treating patients with renal disease. Drugs such as steroids have been used to prevent the progression of renal disease, but they produce toxicity because of their wide distribution in the body. The development of a renal delivery system that selectively carriers drugs to the kidneys is a promising approach for limiting tissue distribution and controlling toxicity. To overcome the problems associated with conventional therapies, bioactive proteins have been conjugated with water-soluble polymeric carriers. Conjugated bioactive protein with polymeric carriers regulate the tissue distribution of bioactive proteins, resulting in a selective increase in its desirable therapeutic effects, and a decrease in undesirable side effects. However, for further enhancement of the therapeutic potency and safety of conjugated bioactive proteins, more precise control of the *in vivo* behavior of each protein is necessary for selective expression of their therapeutic effect. Recently, we reported that the poly(vinylpyrrolidone-co-dimethyl maleic acid) [PVD] was selectively distributed into the kidneys after intravenous injection and it was conjugated with the amino groups of drugs. The conjugates demonstrated high accumulation and retention in the kidneys without any adverse toxicity. In this review, with reference to our recent studies, we propose that bioconjugation with the appropriate polymeric modifier of PVD can be a potential therapeutic agent for various renal diseases.

I. Introduction

In recent years, the clinical applications of bioactive proteins such as cytokines and growth factors have been studied. However, the clinical applications of most of these proteins are limited because of their various side effects (Blick et al, 1987; Rosenberg 1987). Generally, the plasma half- lives of bioactive proteins *in vivo* are very short (Donohue et al, 1983; Bollon et al, 1988; Tanaka and Tokiwa 1990). This necessitates their frequent administration at high dosage in order to obtain sufficient therapeutic effects. Such administration markedly destroys homeostasis, resulting in unexpected side effects. In addition, since bioactive proteins exhibit diverse pharmacological actions in various tissues, it is difficult to selectively obtain only the favorable actions (therapeutic effects). To overcome these problems, bioactive proteins have been conjugated with water-soluble polymeric carriers. We have already reported that polymer conjugation of cytokines typified with tumor necrosis factor-α (TNF-α) interleukin-6 (IL-6), and immunotoxin (IT), with polyethylene glycol (PEG) and polyvinylpyrrolidone (PVP), improved their resistance to proteinase, enhanced their plasma half-lives, and resulted in greater therapeutic potency (Tsutsumi et al, 1997, 2000; Kaneda et al, 1998; Kamada et al, 2000; Yamamoto et al, 2003). We have also shown that conjugation with polymeric carriers regulates the tissue distribution of bioactive proteins, resulted in a selective increase in desirable therapeutic effects, and a decrease in undesirable side effects. However, for further enhancement of the therapeutic potency and safety of conjugated bioactive proteins, more precise control of the *in vivo* behavior of each protein is necessary for selective expression of their therapeutic effect. Thus, there is a need to develop novel

polymeric carriers capable of targeting specific tissue, while PEG and PVP are useful and powerful polymeric carriers for improving the plasma half-lives of proteins.

Renal disease is a serious problem that is on the rise all over the world. According to the Third National Health and Nutrition Examination Survey, about 10.9 million people in the United States have renal disease. (Jones et al, 1998). There is no cure for renal disease, and few strategies are available for prevention. Bioactive proteins such as superoxide dismutase (SOD) and interleukin-10 (IL-10) were believed to prevent the progression of renal disease; however, their therapeutic potency was too low as they were poorly distributed to the kidneys. The development of a renal delivery system that selectively targets the kidneys is a promising approach for limiting tissue distribution and controlling toxicity. Several renal drug delivery systems have been described. One approach involves prodrugs that are cleaved by kidney-associated enzymes to release the drugs in the kidney (Elfarra et al, 1995). However, these prodrugs tend not to accumulate in the kidneys because of plasma protein binding and limited transport to the kidney. Alternatively, low-molecular-weight proteins such as lysozyme have been used as carriers because they are easily reabsorbed by the kidneys. Unfortunately, they also result in considerable renal toxicity and cardiovascular side effects (Haverding et al, 2001). A third strategy has been based on the binding capacity of streptavidin carriers to biotin in the kidney. However, streptavidin is immunogenic and also results in limited renal accumulation because of its large molecular size (Schechter et al, 1995). The fate and distribution of conjugates between polymeric carriers and drugs is determined by their physicochemical properties such as electric charge and hydrophilic-lipophilic balance (Inoue et al, 1989). In this review, at first, we show that PVD is accumulated and retained in the kidney without any adverse toxicity. Additionally to assess the usefulness of PVD as a renal targeting polymeric carrier of drugs, we evaluated the relationship between PVD molecular weight and renal accumulation. We then prepared a conjugated SOD with PVD and evaluated its pharmacokinetic characteristics and therapeutic effects on $HgCl_2$-induced acute renal failure (ARF). This review will provide fundamental information enabling us to design of polymeric drug carriers and its application for renal drug targeting.

II. Pharmacokinetics of PVD

The *in vivo* pharmacokinetics of polymer-conjugated drugs such as bioactive proteins may be markedly influenced by the properties such as electric charge and hydrophilic-hydrophobic balance of polymeric carriers attached to the surface of the drugs. Therefore, in order to optimize drug therapy by polymer conjugation typified by PEGylation, we must initially design a polymeric carrier with useful functions such as targeting and controlled release capability, which can precisely regulate their behavioral characteristics *in vivo*. We reported that PVP was a more suitable polymeric carrier for enhancing the blood residency of drugs than PEG, polyacrylamide (PAAm), polydimethylacrylamide (PDAAm), and polyvinyl alcohol (PVA) (**Figure 1**). PVP, PAAm, and PDAAm could be functionalized by introduction of various comonomers on radical polymerization. PVA has several primary OH groups that can be used for bioconjugation on the side chain. Most appropriately, using this PVP as a backbone polymer, we have evaluated the in *vivo* pharmacokinetics of synthesized PVP derivatives with various electric charges or hydrophilic-hydrophobic balance. We assessed the pharmacokinetic properties of various PVP derivatives. We demonstrated PEGylated TNF-α was improved its anti-tumor effect than native TNF-α in mice bearing tumor, because their blood residency not tumor distribution (Tsutsumi et al, 1995). Among these, carboxylated PVP accumulated in the kidney 24h after intravenous injection (**Figures 2 and 3**). The *in vitro* cytotoxicity of carboxylated PVP against renal tubular cells was low, and its renal targeting capacity

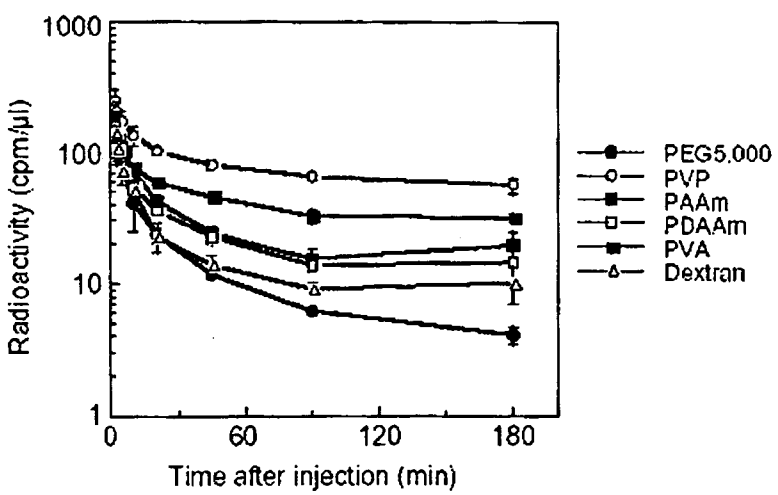

Figure 1. Plasma clearance of various water-soluble polymers in mice after intravenous injection.
From Biomaterials. 2004 Aug;25(18):4309-15

was better than that of other carriers (**Figure 5**). Anionic polyaspartamides are transiently distributed in the kidney and are rapidly excreted in the urine (Rypacek et al, 1982). However, we found that these anionic polymers were not suitable as renal targeting carriers, because the conjugates composed of these anionic polymers and the drug did not accumulate in sufficient quantities to produce therapeutic effects.

We synthesized PVD by radical copolymerization and mixed the reactive comonomers [Dimethyl maleic anhydride (DMMAn) and vinylpyrrolidone (VP)] to evaluate its use as a polymeric drug carrier for renal drug delivery systems. We found that about 80% of the dose of PVD selectively accumulated in the kidneys 24 h after intravenous injection (**Figure 4**). Although PVD accumulated in the kidneys was gradually excreted in the urine, about 40% was retained 96 h after beginning the treatment. The high renal accumulation and retention of PVD makes it a more useful targeting carrier than other agents. Although most anionized polymers are safer than cationized polymers, they exhibit cytotoxicity at high doses. Indeed poly(VP-co-MAn), PVD, which has the same molecular size, polydispersity, and carboxyl group content as PVD, produced cytotoxicity in LLC-MK2 cells at higher concentrations (**Figure 5**). In contrast, PVD produced no evidence of pathological effects in mice at a dose of 10mg/d for 28 d. A subcutaneous dose of 50mg PVD, which had a jelly-like consistency, was well tolerated by mice. The safety of PVD seems similar to that of PEG and PVP, which are used clinically. Thus, PVD seems to be a safe polymeric carrier with much higher renal targeting and retention capacity than any other renal targeting carrier. PVD was hydrolyzed at the maleic anhydride position to form carboxyl group, which produced polyanionic characteristics. Endothelial cells and the glomerular capillary wall are coated with highly polyanionic sialprotein (Simionescu, 1983). Therefore, anionic polymers such as anionized dextran are generally cleared more slowly from the circulation than are nonionic and cationic polymers (Chang et al, 1975). The reason for this discrepancy *in vivo* activity is not clear. In a preliminary study, the uptake of PVD by renal cells was inhibited by the energy inhibitor NaN_3 and was not affected by cytochalasin B.

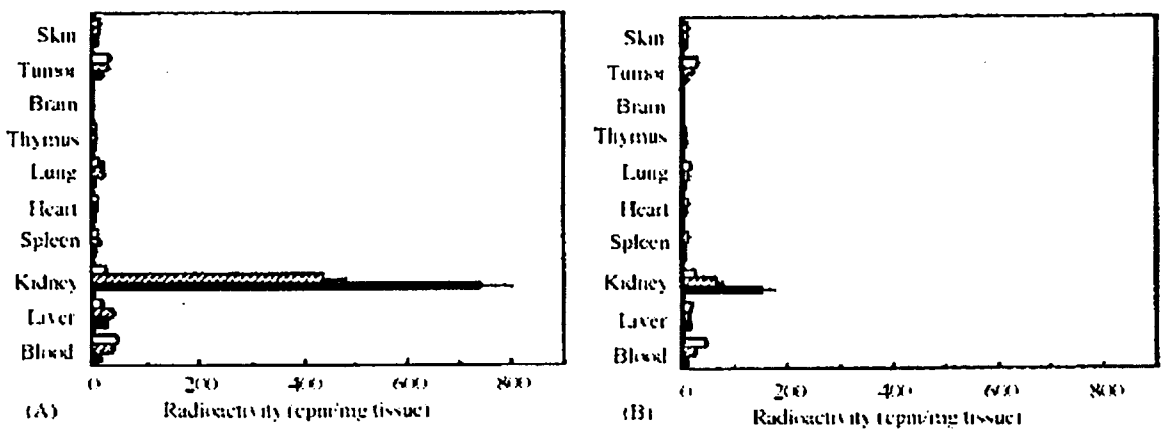

Figure 2. Tissue distribution of PVP and anionized PVP derivatives at 3h after intravenous injection in mice.
From Biomaterials. 2004 Aug;25(18):4309-15

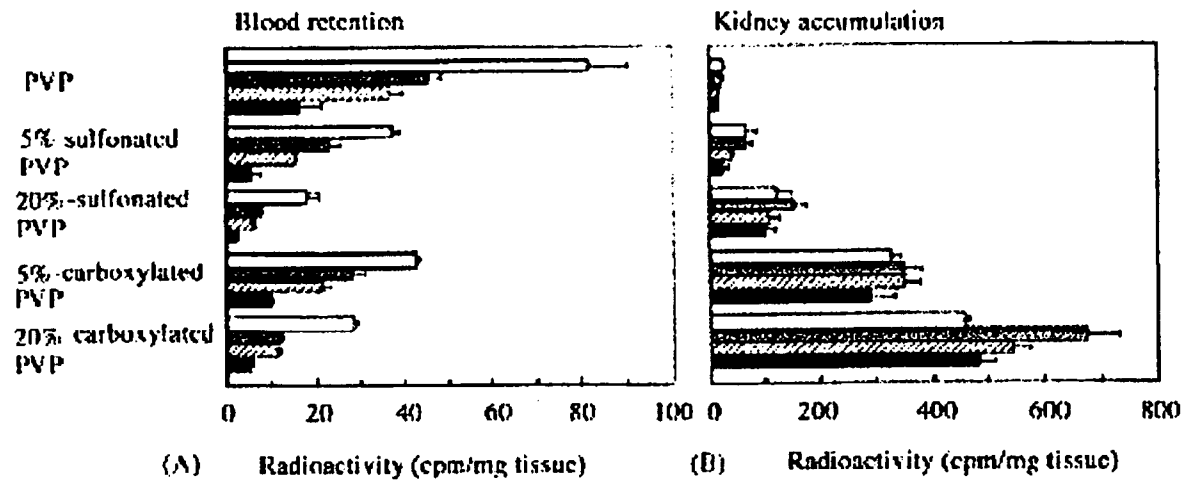

Figure 3. Blood retention and kidney accumulation of PVP and anionized PVP derivatives after intravenous injection in mice.
From Biomaterials. 2004 Aug;25(18):4309-15.

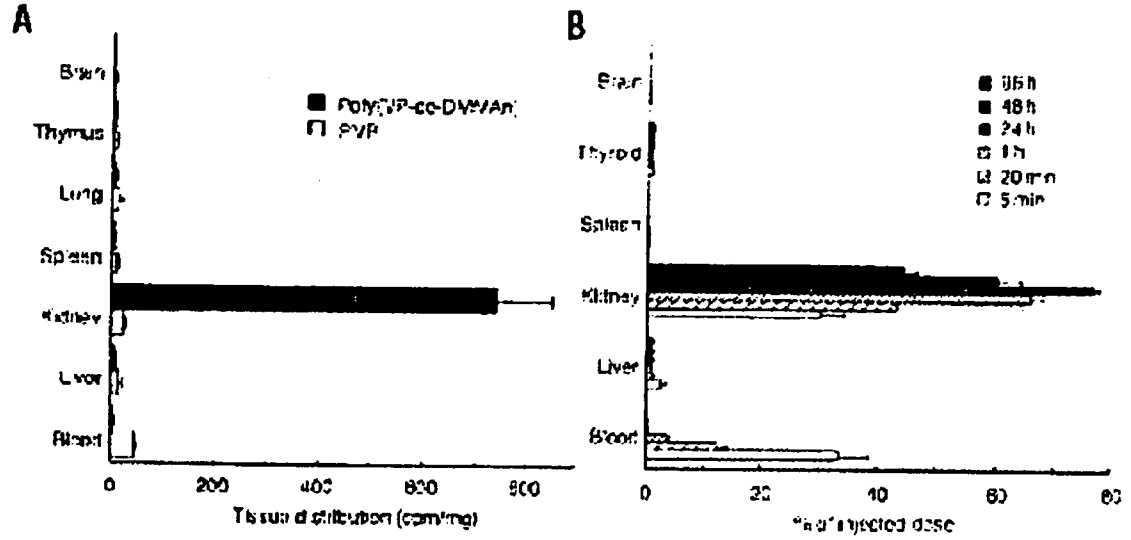

Figure 4. Tissue distribution of PVD after intravenous injection.
From Nat Biotechnol. 2003 Apr;21(4):399-404

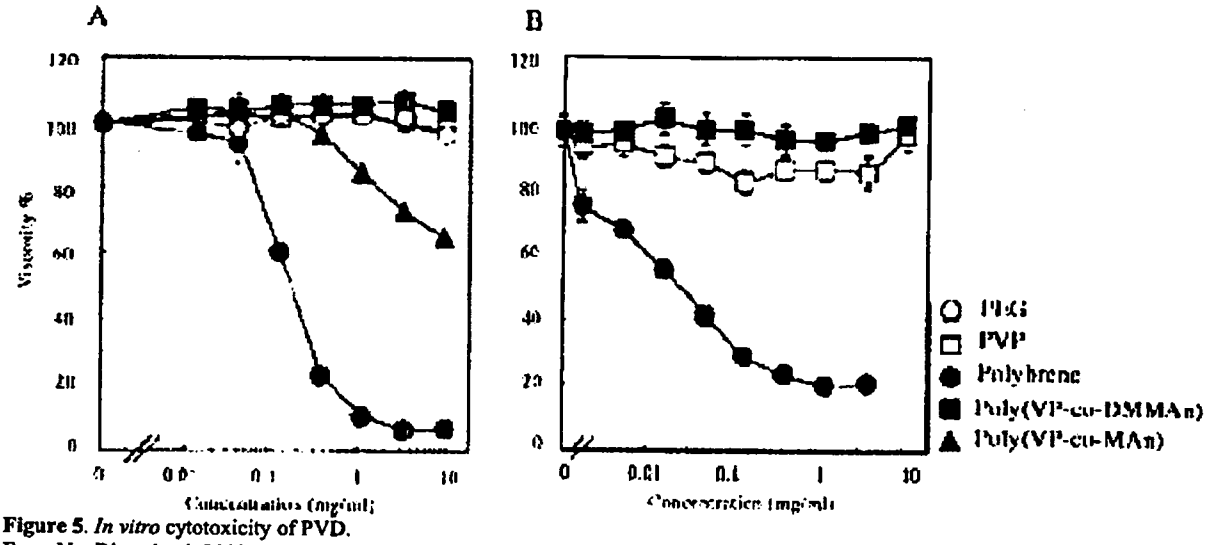

Figure 5. *In vitro* cytotoxicity of PVD.
From Nat Biotechnol. 2003 Apr;21(4):399-404

Thus, PVD may be taken in by an energy-dependent process other than endocytosis. Several specific molecules are involved in renal transport, and various organic anion transporters exist in the kidney (Moestrup et al, 1996; Sweet et al, 1997; Hosoyamada et al, 1999; Nakajima et al, 2000). However, these transporters generally carry low molecular weight drugs. Therefore, a new transport pathway may exist. It is important to consider the *in vivo* uptake pathway (reabsorption pathway or direct pathway) of PVD into the proximal tubule. We found that the *in vivo* behavior of PVD was similar in both normal and ARF mice. Since reabsorption did not occur in ARF mice, we believe that PVD was delivered directly to the proximal tubule.

We injected mice intravenously with fluorescenly labeled PVD and collected their kidneys after 3 h. We prepared sections and evaluated them by fluorescence microscopy (**Figure 3**). Most of the PVD accumulated in the cortex (data not shown). PVD was also present in renal tubules, especially proximal tubular epithelial cells, but not in glomeruli. In contrast, fluorescence-labeled PVP did not accumulate in the renal tubules. Neither amino-aceto-fluorescein nor the mixture with hydrolyzed PVD was detected in renal tubules.

Further we used ^{125}I-tyramine and amino-aceto-fluorescein as model drugs with low molecular weight, and showed that they specifically accumulated in the kidney after conjugation with PVD (data not shown). PVD may serve as a carrier for site-specific delivery of drugs with relatively low molecular weight to the kidney. These drugs may include radionucleotides or anti-inflammatory drugs, antibiotics, and other effector molecules. Furthermore, DMMAn is an amino-protective agent that binds to or separates from amino groups when the pH changes (Nieto and Palacian, 1983; de la Escalera and Palacian, 1989; Kaneda et al, 1998). PVD also has maleic anhydride groups that react with amino groups in drugs. In inflammatory tissue and tumor tissue, the pH is lower than

normal (Nakajima et al, 2000). Therefore, if PVD is used in nephritis and renal cancer, it is expected to accumulate in the kidneys and gradually release the drugs. In addition, the modification of proteins with polymeric modifiers has several advantages. TNF-α, IL-6, and functional single-chain Fv fragment bioconjugated with PEG or PVP are more effective than the native proteins (Tsutsumi et al, 1995, 1997, 2000; Kamada et al, 1999, 2000; Mu et al, 1999; Tsunoda et al, 2000, 2001). We have also shown that the fate and distribution of proteins with polymeric modifiers are strongly influenced by the polymeric modifiers. Therefore, PVD may be a useful modifier of bioactive proteins for targeting the kidney.

III. Therapeutic effect of PVD-SOD

We synthesized PVD as a new renal targeting carrier. About 80% of the dose of PVD was selectively distributed to the kidneys after intravenous injection and then gradually excreted through urine. Approximately 40% remained in the kidneys 4 days after the intravenous injection (**Figure 4**). No side effect occurred in the kidney and other tissues by administration of excessively high dose of PVD. Next, we assessed the usefulness of PVD as a renal targeting carrier. The relationship between the M_n of PVD and its renal accumulation after intravenous injection was investigated. To evaluate the influence of molecular weight on renal accumulation of PVD, we estimated the plasma clearance and tissue distribution of PVD with various M_n after intravenous injection (**Figure 7**). The radioactivity in the supernatant of homogenized kidneys was measured after acid precipitation to distinguish between bound polymer and free tyramine, it was confirmed that the PVD did not release the free tyramine and it was not degraded in the kidneys (data not shown). The blood retention increased as the molecular weight increased (**Figure 7A**). On the other hand, PVD with an average molecular weight of 6–8kDa (PVD_{6k} and PVD_{8k}) showed the highest renal accumulation and about 80% of the administered dose accumulated in the kidneys at 3 h after injection (**Figure 7B**). Accumulation rates decreased to 60% for PVD_{14k} and 30% for PVD_{3k}. We examined the clearance, which was calculated on the basis of radioactivity at 3 h after intravenous injection of various PVDs in mice (Nishikawa et al, 1996; Nishikawa et al, 2003). The uptake clearance of PVD_{6k} was the highest among various PVDs. PVD_{6k} and PVD_{8k} were rapidly eliminated from the blood and specifically accumulated in the kidneys only 1 h after intravenous injection without being distributed to other tissues.

In addition, PVD_{6k} and PVD_{8k} showed high retention in the kidneys and about 60% of the injected dose was retained in the kidneys 24 h after intravenous administration. By the measurement of the urinary radioactivity excretion, it became clear that the PVD which accumulated in the kidney was gradually excreted through the urine. Furthermore, measurement of urinary radioactivity excretion revealed a significantly higher value for PVD_{3k} with the lowest molecular size (**Figure 8**).

We further evaluated the usefulness of PVD as a renal targeting carrier by polymer conjugation to SOD, which is viewd as a potential drug for renal disease. Several recent studies have reported an association between activated oxygen species such as superoxide

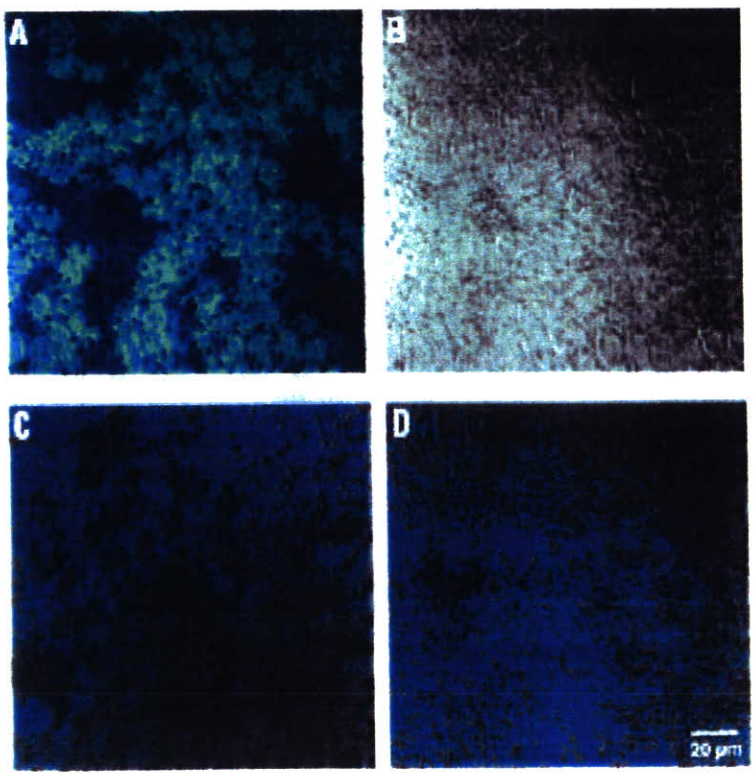

Figure 6. Histological sections of renal tissues in mice receiving an injection of fluorescein-labeld PVD.
From Nat Biotechnol. 2003 Apr;21(4):399-404

radical, hydrogen peroxide hydroxyl radical, and NO with various pathologic diseases processes such as cancer, inflammation, septicemia, and necrosis associated with ischemic reperfusion. Several studies have investigated the use of activated oxygen metabolic enzymes and antioxidants as therapeutic agents in diseases where stress oxidation plays a prominent role. SOD has shown promise as a therapeutic agent capable of eliminating superoxide radical in the early stages of formation of highly reactive oxygen species such as hydroxyl radical. Developments in genetic engineering have now enabled the production of large quantities of human Cu/Zn-SOD, which has attracted attention as a therapeutic agent. Hashida et al. reported that cationized SOD and PEGylated SOD exhibited significant therapeutic effects on ischemic acute renal failture (Fujita et al, 1992; Mihara et al, 1994). However, there is no report as to delivery of drug to the kidney specifically. With respect to kidney disease, activated oxygen is known to play an indispensable role in the mechanisms of ARF, complications associated with long-term maintenance dialysis, drug toxicity, and various inflammatory conditions. The PVD-SOD was prepared via formation of amide bound between the SOD lysine residues and carboxyl groups of PVD_{6k}. The resultant PVD-SOD was separated into three fractions of different molecular sizes (high = H, middle = M, low = L) by gel filtration HPLC, and then, specific activities were measured. The separated PVD-SODs, with molecular sizes of 73, 120, and 220 kDa, were termed L-PVD-SOD, M-PVD-SOD, and H-PVD-SOD, respectively. Although specific activity decreased with an increase in the molecular size, even H-PVD-SOD with the largest molecular size still had 60% activity compared with native SOD.

We then evaluated the pharmacokinetics of the three kinds of PVD-SODs after intravenous administration. Native SOD was rapidly cleared from the blood circulation (**Figure 9A**) 3 h after injection, accumulation of native SOD into the kidneys was observed in small quantities (**Figure 9B**), and almost all native SOD was found to be eliminated in the urine (data not shown). On the other hand, the blood residency and renal distribution

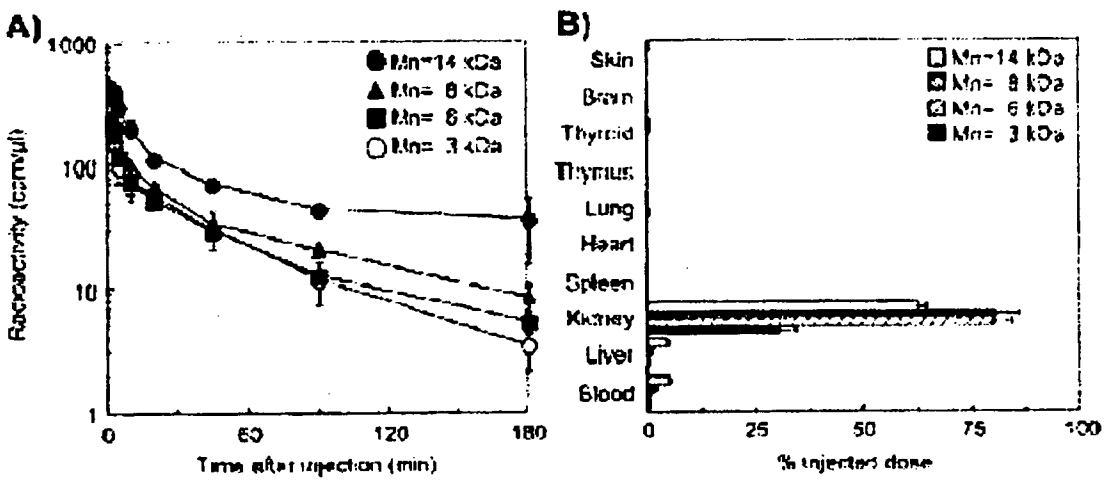

Figure 7. Plasma clearance and tissue distribution of PVDs with various molecular weight (M_n) after intravenous injection. From J Control Release. 2004 Mar 5;95(2):229-37.

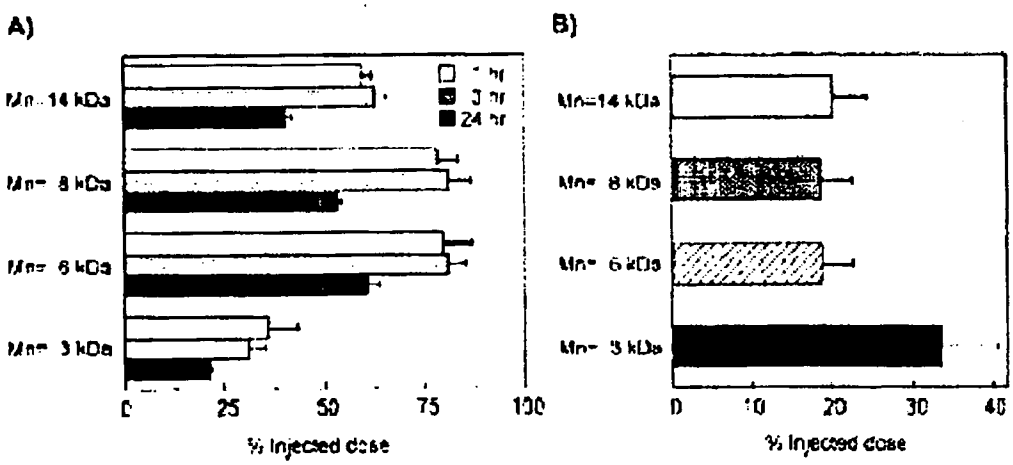

Figure 8. Renal accumulation and urinary excretion of PVD with various molecular weight after intravenous injection. From J Control Release. 2004 Mar 5;95(2):229-37